Loess in the Tian Shan and its implications for the development of the Gurbantunggut Desert and drying of northern Xinjiang

FANG Xiaomin[1,2], SHI Zhentao[1,3], YANG Shengli[1], YAN Maodu[1,4], LI Jijun[1] & JIANG Ping'an[5]

1. National Laboratory of Western China's Environmental Systems of Ministry of Education of China & Department of Geography, Lanzhou University, Lanzhou 730000, China;
2. State Key Laboratory of Loess and Quaternary Geology, Institute of Earth Environment, Chinese Academy of Sciences, Xi'an 710054, China;
3. Institute of Cold and Arid Region & Environment and Engineering of Chinese Academy of Sciences, Lanzhou 730000, China;
4. Department of Geological Sciences, University of Michigan, Ann Arbor, MI 48103, USA;
5. School of Agriculture, Xinjiang Agriculture University, Urumqi 830000, China

Abstract **Eolian loess is widely distributed on the various geomorphic surfaces between 700—2400 m a.s.l. on the northern slope of the Tian Shan. It is formed in a synchronous manner with dust transported from the Gurbantunggut Desert in the Junggar Basin. The thickest section of loess was found in the Shawan and Shihezi regions. Paleomagnetic and climatic proxy analyses of over 71 m of a loess-paleosol sequence on the highest terrace of the Qingshui He (River) in the Shawan show that the paleomagnetic Bruhues/Matuyama (B/M) boundary lies at the bottom of paleosol S8, at a depth of 69.5 m, and the bottom of the sequence was estimated to be ~0.8 Ma. This implies that the extremely dry climatic conditions in the Junggar Basin and the initial Gurbantunggut Desert were present at least by 0.8 Ma. High-resolution grain size series demonstrate that this area and desert expansion experienced two dramatic periods of desert expansions that occurred at ~0.65 Ma and 0.5 Ma, respectively; and the subsequent continuous enhancement led to the environment presently observed. This tremendous environmental effect, caused by large-scale expansion of the desert and arid region of inner Asia, might be an important driving force for the global temperature drop that occurred in the mid-Pleistocene.**

Keywords: Tian Shan loess, Gurbantunggut Desert, aridification, global change.

The mid-latitude temperate arid region that is largely observed in the Asian inland and Midwestern America, are characteristic of non-zonal landscapes. These regions occupy an area of 708 million hectares, accounting for 45% of the total arid regions on earth. They formed in different geologic times and in conditions ranging from tropical to sub-tropical arid regions due to a sub-tropical high. They are largely due to increasing continental mass and aridity caused by continental accretion and uplifted orogeny from plate collision. It is postulated that prominent fluctuations occurred within these arid regions. The resultant environmental effects (e.g. changes in albedo and dust) might have been the cause for major influences on global climatic change[1—4]. The Asian arid inland is main part of the global temperate arid region; and the major component of this region is northwestern China. The latter has an area of 157 km^2 and produces ~800 million tones of dust per year, which accounts for 50% of the world's total annual dust supply[1,5]. About 50% of China's inland dust are transported outside the Chinese mainland to the Pacific Ocean[6,7] and even farther to western North America, Greenland and the Arctic[8] by winter monsoons and some annual westerlies. Especially during glacial periods, not only does the amount of dust increase by 3—4 times more than present[9], but also the area of arid to sub-arid regions increases significantly[10], latitudinally expanding southward by ~8° to regions south of the Yangtze River[11], and longitudinally, to the east by ~20° to about 125° E with a horizontal distance of nearly one thousand kilometers[12]. This great change in Asia's arid region and its environmental effects are predicted to have a great impact on the global climatic change[1—4]. But before discussing the significance of this change to climatic variations, and what the mechanisms are, much work should be done to clarify them in two levels. One is the evolution of the arid region, especially to demonstrate and establish the great arid environment-dust series, then to examine its relation with local and global climate change events and their mechanisms. Finally, advanced atmospheric numeric circulation models are reviewed to examine their effectiveness.

Much qualitative work has been carried out on the evolution of the arid region in northwestern China. Recent high-resolution semi-quantitative studies on the stratigraphy and paleoclimate in the Linxia Basin, Gansu Province over the last 29 Ma and the existence of the red clay-loess sequences demonstrate that the arid environment linked to the arid region of NW China might have appeared in 8—9 Ma[13—17] and reached its present scale after long complicated processes and a general expansion trend, especially after the great expansion during the mid-Pleistocene[18]. This arid expansion may have had a close relationship with the uplift of the Tibetan Plateau.

However, the studies mentioned above provide just a rough framework. To establish a detailed framework of evolution of the desert and arid regions, reconstruction of the evolutional histories of several main deserts in northwestern China is crucial, together with an understanding of general conditions of aridity from red clay-loess records on the Loess Plateau. Our preliminary studies on loesses on the northern slopes of the Kunlun Shan and the Qilian Shan show that conditions like the present Taklimakan Desert and Badain Jaran Desert were initiated

about 0.8—0.9 Ma ago, followed by two rapid expansions at ~0.5 and ~0.14 Ma, and continued expansion to finally reach its present scale[18,19]. If our postulate is correct, the adjacent Gurbantunggut Desert in the Junggar Basin should have been initiated at roughly the same time and should have experienced a similar evolution history. Hence, we chose the loess on the northern slope of the Tian Shan, which is formed from the synchronous deposition of the Gurbantunggut Desert dust, to suggest a desertification history of northern Xinjiang and the evolution of this desert region, with the ultimate objective of understanding their relationship with the local and global climate change.

1 Physiographic setting

The studied area is located between the Dushanzi and the Hutubi on the northern slope of the middle Tian Shan (fig. 1). There are extensive loess deposits on varying geomorphic surfaces (e.g. terraces and foothills) between 2400 and 700 m a.s.l. along the southern margin of the Junggar Basin and below the fir-spruce forest on the northern slope of the Tian Shan. This has produced the impressive NWW foothill loess zone (fig. 1). The regional thickness of the loess is between 5—30 m around this region, but it can be as thick as between 30—50 m and it even reaches up to ~90 m thickness in the Shihezi. To date, it is the thickest observed loess deposit in the northern Tian Shan region. The loess thickens away from the Junggar Basin to the south and pinches out further south when near the Tian Shan. Little to no loess is deposited above the forest line. Particle grain size of the loess and other eolian sediments show a corresponding trend in fineness. Grain size distribution of the eolian sediments formed the apparent desert, loessy sand and loess zones, respectively (fig. 1). To the west of the Hutubi, the Desert is characterized by NW trending barchan dunes and chains, as well as longitudinal dunes or their composites; and to the east are the NNE-SSW trending longitudinal dunes and composite barchan chains. The specific distribution of the loess and desert dunes indicates that there are two major wind directions in the region. These major wind currents are the NW winds, coming from the wind currents over the passes of northern stretch of the Tian Shan

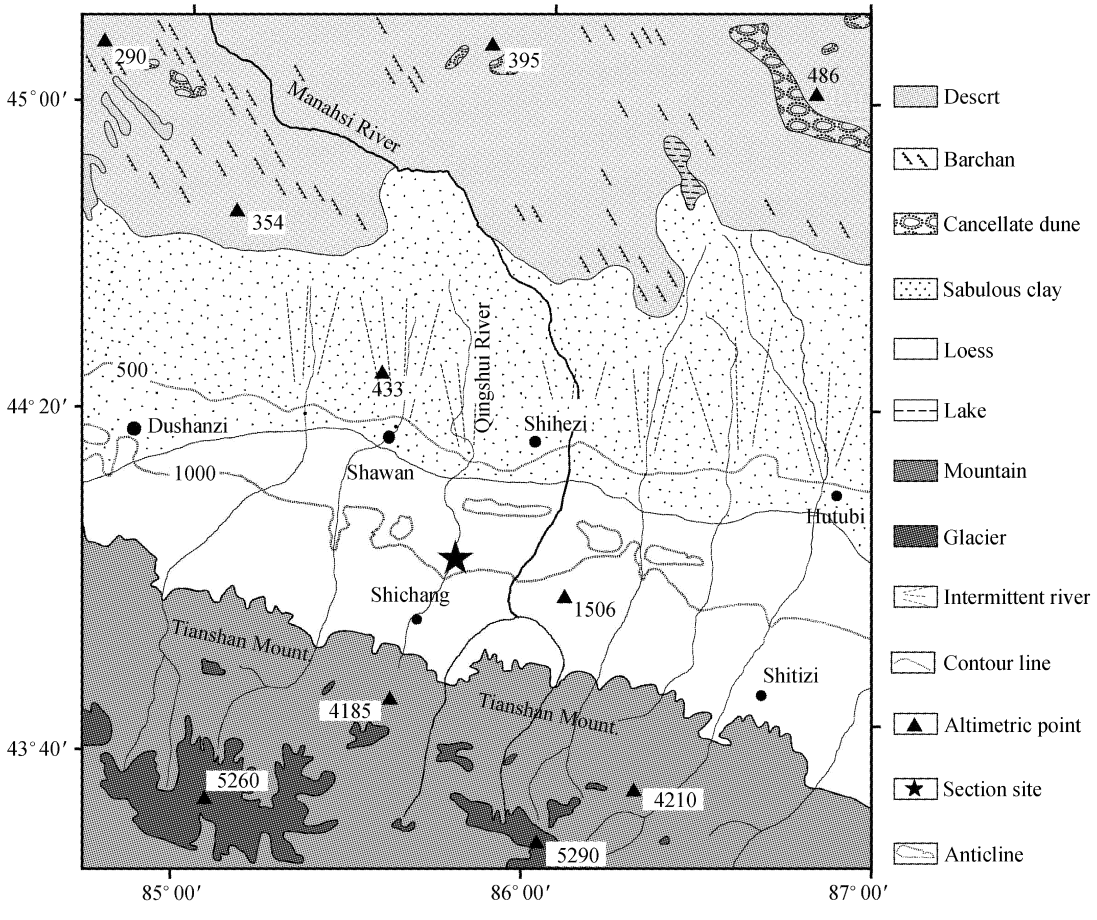

Fig. 1. Geomorphology and distribution of loess in the studied area.

(e.g. the well-known Alashan Pass and Laofengkuo Pass), that correlate to the NW trending barchan dunes; and the NNE winds, from the currents over the paleo-Wulun River valley between the Artai Shan and the northern stretch of the Tian Shan. These correlate with the NNE dune set and are a product of the southward topography and the Mongolia high. As shown in the mean annual atmospheric circulation diagram, these currents are mainly formed by flowing Westerlies around the northern slope of the Tian Shan, and are obviously affected by the Mongolia high to east region of the basin. That may be the reason for the thickest loess being deposited in Shawan, where the two currents meet.

Previous studies have suggested that only a small amount of loess has been deposited on the northern slope of the Tian Shan, and its maximum thickness is only of the magnitude of tens of meters. It is believed to be late Pleistocene in age[22]. Since the 1980s, some studies have demonstrated that these loess deposits were mainly of eolian origin and were correlated with the Lishi loess on the Loess Plateau. Hence the oldest loess might be L4[23,24]. Because of the uncertainty associated with thermoluminescence (TL) dating of old stratum, the age and environmental significance of northern Xinjiang loess has never been highlighted. Therefore, we have concentrated our work in this region mainly on obtaining the age of the oldest loess in northern Xinjiang and delineating the climatic records from some main climatic proxies.

2 Locality and stratigraphy

The studied section is located on the sixth-stratigraphically highest terrace ~2 km SW of the Dongwan Town, Shawan County (fig. 1). The erosional top of the terrace is at 860 m elevation, and consists of 71 m loess and loessic sands with a gravel bed at the bottom, in which the base is not exposed. At a depth of 9.8 m, 38 m and 53 m, respectively, the section can be divided into 4 layers as the uppermost, upper, lower and the lowest. The uppermost layer is characterized by loose texture, dark yellow color and massive structure, with many biological channels. The upper layer is of light brownish yellow color and tight massive structure, with many intercalated greenish yellow-greenish gray loessic sands, with decreasing frequency below 16.7 m. The lower part is identified as dark brownish yellow in color with a massive tight structure, and is observed to contain grayish yellow loessic sand with ripple bedding or cross bedding. The lowest layer is light brownish gray in color and of tight structure. This unit contains some distinct small carbonate nodules or filled pores, and is observed to have weak ripples or cross bedding structures that increase in frequency below 60 m. Although the paleosols are weakly developed, nine layers of paleosol complexes have been identified, marked as S_0—S_8 after conventional paleosol numbering used in the Chinese Loess Plateau (fig. 2). The S_0, S_1 and S_5—S_8 features show relatively strong development, are of brownish gray or brown color and massive structure, with many biological channels, carbonate spots and small nodules. The soil profile is rather weak. The other paleosols are relatively weak, of light brownish gray color, with less biological channels and carbonates; there is no distinct carbonate layer in the soil profile. In general, with a boundary set at 38 m, the paleosols in the lower portion are more developed than those in the upper portion (fig. 2).

3 Sampling and laboratory analysis

Samples were collected along a 1.5—3-m-deep trench dug in the section and a 5-m-deep well down to the top of the river gravel layer. Paleomagnetic samples were collected at 1 m intervals in 0—55 m and at 0.5 m intervals in 55—71 m. Three oriented specimens of 2 cm × 2 cm × 2 cm were collected at each level, yielding a total of 255 specimens. Bulk samples were taken at 5 cm intervals for measurements of grain size, yielding a total of 1420 samples. Grain sizes were measured on the American Mastersizer 2000 laser particle sizer (analytical range: 2 mm—0.02 μm) with errors less than 1% at the National Laboratory of Western China's Environmental Systems (LWCES) of the Ministry of Education of China, Lanzhou University. ^{14}C-dating of organic fractions was performed in the Institute of Cold and Arid region & Environment and Engineering of CAS, and TL dating was carried out at the Institute of Earth Environment of CAS. Paleomagnetic samples were measured at the Paleomagnetism and Environmental Magnetism Laboratory of the LWCES. The specimens were demagnetized in the American TD-48 (thermal demagnetometer, ASC company), and the remnant magnetizations were measured on a Czeck JR-5A high-resolution spinner magnetometer (AGICO company). To best eliminate the effect of the Earth's field, the exit of the thermal demagnetometer and the measuring place of the spin magnetometer are placed in the center of a Helms magnetic shield (counteract magnetic field less than 20 mG within a 20 cm radius).

4 Paleomagnetic results

The representative specimens of loess and paleosol were selected and 18-stepwise demagnetized from room temperature to 685℃. Most of the specimens show a similar trend. The intensity and direction of the remnant magnetization show a significant variation at ~200℃, suggesting removal of the viscous remnant magnetization (VRM). After 300℃, a magnetic component with a stable direction pointing to the origin of the Zijderveld coordinates is observed, and its intensity decreases gradually with increasing temperature. Hence, this is the stable

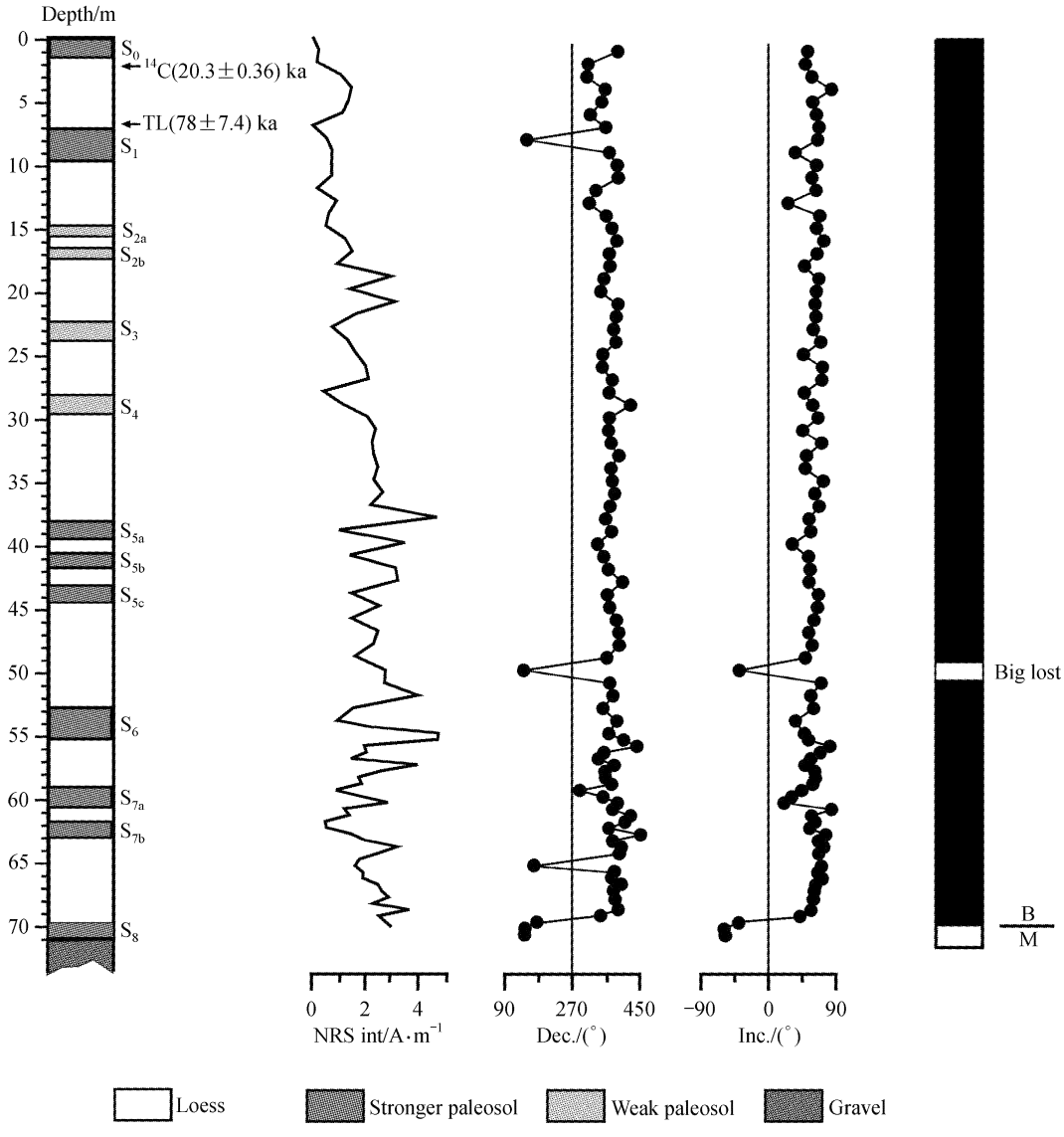

Fig. 2. The lithology and magnetostratigraphy of the Dongwan loess section on the northern slope of the Tian Shan.

characteristic remnant magnetization (ChRM). Only a few coarse grain specimens have low remnant magnetization, but their directions are unstable. Therefore, all the other specimens were demagnetized by only 3—4 steps between 300—550℃. We obtained the direction of the ChRM by main component analysis. For unstable specimens and the lowest 5-m specimens, we remeasured their 18-step thermal demagnetization results on the 2G cryogenic magnetometer in the completely shielded paleomagnetic laboratory of Department of Geological Sciences, University of Michigan. The lowest 5-m specimens show similar results, and the unstable specimens also present stable directions. We suggest that the precision and the degree of shielding are not high enough to measure the weak remnant magnetization specimens. All the data are shown in fig. 2 after fisherian average are carried out.

Clearly, almost all normal directions are observed above a depth of 69.5 m, except for one brief reversal at a depth of 50 m. All samples below a depth of 69.5 m have reversed directions. The development of the Holocene topsoil S_0 and the last interglacial paleosol S_1 at 9 m, as determined respectively by ^{14}C dating of organic material and TL dating (fig. 2), has demonstrated that the loess deposited continuously to the present. Because of the similar character and stratification of the loess-paleosol sequences from field identification and laboratory grain size analysis, together with the B/M boundary which also

appears in loess L8 on the Loess Plateau, we correlate the section above a depth of 69.5 m with the Brunhes normal polarity chron and the section below this depth with the uppermost Matuyama reversed polarity chron. Using a mean depositional rate of 9.16 cm/ka from the bottom age of S_1 to the B/M boundary or of 8.9 cm/ka of the Brunhes section, the age at 50 m depth is about 567 or 561 kaBP. This brief reversal in the Brunhes chron may be a record of the paleomagnetic "Big Lost Event" at (565 ± 14) kaBP[25]. The age of the paleosols, which are calculated by magnetostratigraphy, are close to those on the Loess Plateau; the bottom age of the section is also close to our recent results from the northern slope of Kunlun Shan[18]. Hence, our age interpretation fits reasonable expectations.

5 Drying of northern Xinjiang and the formation and evolution of the Gurbantunggut Desert

Fig. 3 shows the magnetic susceptibility variations and grain size results for the section. It can be seen that both the two climatic proxies shifted at a depth of 53 m (on the top of S_6, ~ 0.65 Ma) and 38 m (on the top of S_5, ~0.50 Ma); the grain size apparently became coarser, especially at 38 m. The content of coarse fraction > 63 μm and the mean grain size, which represent the aridity and the atmospheric circulation / strength of wind, respectively, increased from 8.3% to 9.0% up to 15.4% and from 25.8 μm to 26.8 μm up to 34.7 μm; while those with the contents of grain size < 2 μm, which indicate the intensity of pedogenesis, decreased from 8.6% to 6.8% and to 6.5%. We suggest that these two environmental events may represent the two main increasing aridity and atmospheric circulation enhancing events in northern Xinjiang.

Regional deposition of loess is synchronous with the formation and evolution of deserts. Hence, the appearance of the northern Xinjiang loess at ~0.8 Ma may demonstrate the rapid drying of the Junggar Basin and the forming of the initial modern Gurbantunggut Desert; meanwhile, it also suggests the appearance of atmospheric circulation similar to the present. Then, at ~0.65 Ma and 0.50 Ma, the drying of northern Xinjiang and the changing of atmospheric circulation were further enhanced, with the desert expanding rapidly. Finally, with continuous drying, the modern Gurbantunggut Desert and the environment pattern in northern Xinjiang were formed. The arid environment in northern Xinjiang and the evolution of the desert are affinitive to the arid environment in southern Xinjiang and the evolution of the Taklimakan Desert, which have been demonstrated by Kunlun Shan loess[18]; they are also synchronous with the enhancement of the Asian winter monsoon and dry-cold events, which are reflected in the appearance of the NE Tibetan loess and its coarsening grain size. This suggests that both the emergence of an extreme dry climate and large-scale deserts in inland northwest China happened much later than what has previously postulated, especially since the enhancement of drying and expansion of desert are synchronous with events such as mid-Pleistocene global climate chilling, the increasing amplitude of glacial-interglacial climate oscillations and shifting of periodicity of climatic change, together with the distinct enhancement of the strength of winter-summer monsoon conditions since ~0.8 Ma, which is represented by grain size and susceptibility of loess-paleosol sequences on the Loess Plateau. We believe that the coupling of these local and global scale synchronic events must have been driven by outside mechanisms; we suggest that the abrupt uplift of the Tibetan Plateau in the mid-Pleistocene entered the cryosphere and caused the mid-lower Westerlies notably bifurcated and byflew around the Plateau, producing further enhancement. These mechanisms are postulated to have caused inland northwest China to rapidly dry, expanding the desert, and forming the present desert and arid environment pattern[18,28]. The previous drying, which was caused by ocean-continent variations and the low altitude uplift of the Plateau, might be weak; hence, grassland vegetation and fauna expanded in the late mid-Pleistocene to early Quaternary northwest China[13], and formed the weak monsoon red-clay and the Wucheng loess[14−17]. These weak arid environments are fundamental to the formation of the mid-Pleistocene drying climate and the initial deserts. The evolution of large-scale deserts in northwest China inland in the mid-Pleistocene and the expansion of the arid region, which must have significantly enlarged the albedo and atmospheric dust flux, have caused the cold climatic events and followed the glacial-interglacial periods. The scale of arid areas and the dust flux have changed over thousands of kilometers and several time differences, and their distinct environmental effects may have magnified the global glacial-interglacial periods together with the amplitude of the Asian monsoon. Hence, the expansion of the Asian arid inland, caused by uplift of the Tibetan Plateau, is postulated to be one of the driving forces of global and local climate change since the mid-Pleistocene.

6 Conclusions

Tian Shan loess formed at ~ 0.8 Ma, roughly reflecting a synchronous appearance of the present-like air circulation system and an extreme dry climate in the Junggar Basin which led to the development of the Gurbantunggut Desert.

There were two-time distinct enhancements of drying events at ~ 0.65 Ma and 0.50 Ma in northern Xinjiang, then a gradual development of the present desert and arid environmental pattern.

The uplift of the Tibetan Plateau is the fundamental driving force for the extreme dry climate in the northwest China inland and the development of the deserts. The distinct increase of the mid-Pleistocene arid region in area

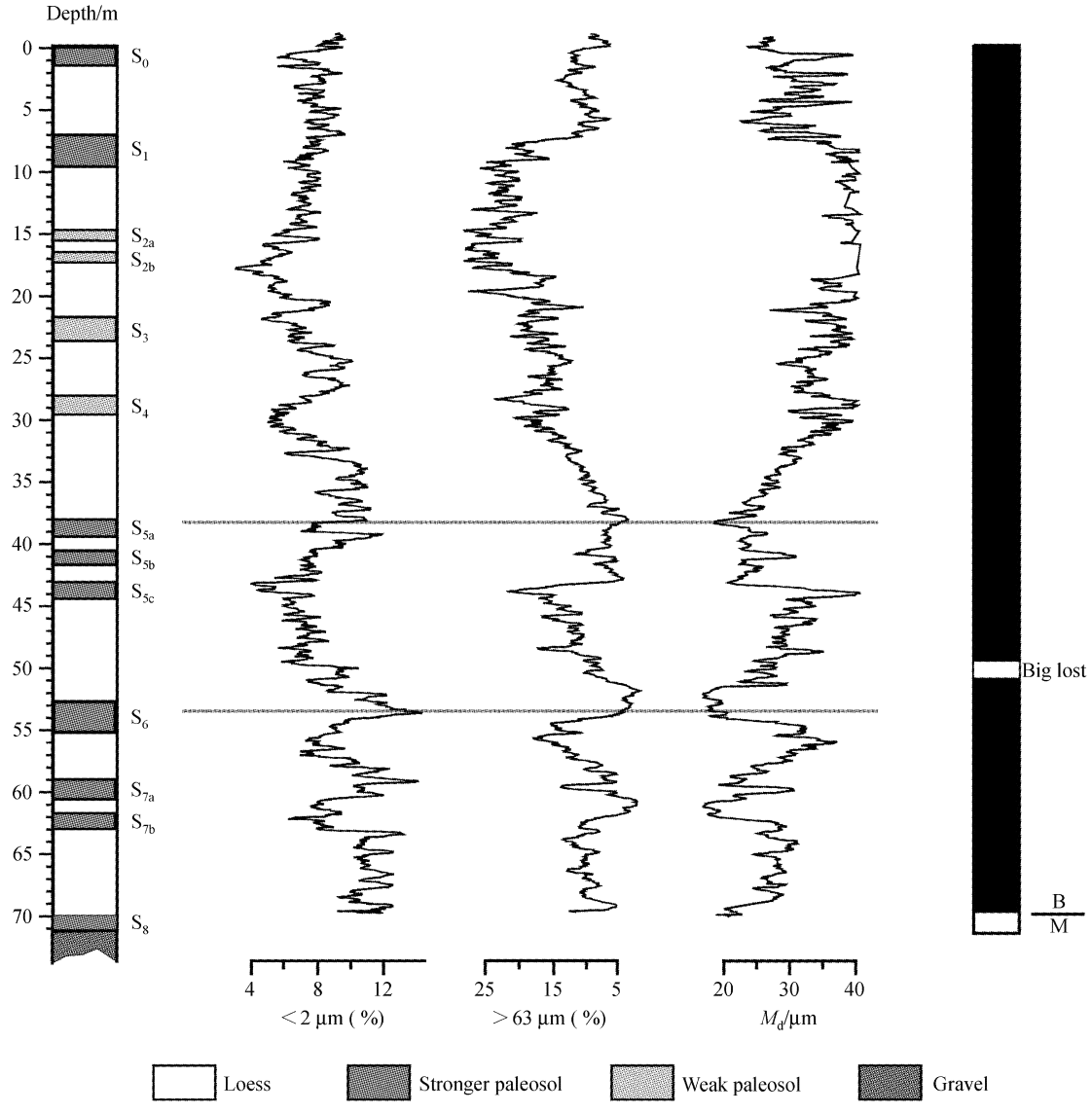

Fig. 3. Grain size curve of the Dongwan loess section in Shawan County.

and occurrence of dust, with high frequency changes with the glacial-interglacial periods may be one of the main driving forces for global chilling, together with increasing amplitude and periodic shift in climate.

Acknowledgements We thank Dai Shuanger and Guo Zhilong for field assistance, Dong Ming for some diagram drawing. Thanks should be also due to Prof. Dong Guangrong for his helpful suggestions and comments on the manuscript. This work was co-supported by China's 'Excellent Researchers Fund' of the National Natural Science Foundation of China (Grant No. 49928101), 'Hundred Talents Project' of the Chinese Academy of Sciences (Renjiaozi[2000]005) and the National Tibetan Project (Grant No. G1998040802).

References

1. Andreae, M. O., Climate effects of changing atmospheric aerosol levels, World Survey of Climatology, Future Climates of the World, Volume 16 (eds. A. Henderson and A. Sellers), Amsterdam: Elsevier, 1995, 341—392.
2. Harvey, L. D. D., Climatic impact of ice-age aerosols, Nature, 1988, 334: 333.
3. Martin, J. H., Glacial-interglacial CO_2 change: the iron hypothesis, Paleoceanography, 1990, 5: 1.
4. Shine, K. P., P. M. de F. Forster, The effect of human activity on radiative forcing of climate change: a review of recent developments, Global and Planetary Change, 1999, 20: 205.
5. Zhang, X. Y., Arimoto, R., An, Z. S., Dust emission from Chinese desert sources linked to variations in atmospheric circulation, J. Geophys. Res., 1997, 102: 28041.
6. Duce, R. A., Liss, P. S., Merrill, J. T. et al., The atmospheric input of trace species to the world ocean, Global Biogeochemical Cycles, 1991, 5: 193.
7. Rea, D. K., The paleoclimatic record provided by eolian deposition in the deep sea: the geologic history of the wind, Reviews of

Geophysics, 1994, 32: 159.
8. Biscaye, P. I., Grousset, F. E., Revel M. et al., Asian provemance of glacial dust (stage 2) in the Greenland Ice Sheet Project 2 Ice Core, Summit, Greenland, J. Geophys. Res., 1997, 102: 26765.
9. Zhang, X. Y., Arimoto, R., An, Z. S., Glacial and interglacial patterns for Asian dust transport, Quat. Sci. Rev., 1999, 18: 811.
10. Dong, G. R., Jing, J., Gao, S. Y. et al., The Climate Change in North China Deserts since Late Pleistocene, Quat. Sci. Res. (in Chinese), 1990, 3: 213.
11. An, Z. S., The Quaternary Loess Geology and Global Change (2) (in Chinese), Beijing: Sci. Press, 1990.
12. Sun, J. M., Ding, Z. L., Liu, T. S. et al., Desert distributions during the glacial maximum and climate optimum: example of China, Episodes, 1998, 21: 28.
13. Li, J. J., Fang, X. M., Uplift of Qinghai-Tibetan Plateau and Environmental change, Chin. Sci. Bull., 1998, 44 (23): 2217.
14. Sun, D. H., Liu, T. S., Cheng, M. Y. et al., Magnetostratigraphy and paleoclimate of red-clay sequences from the Chinese Loess Plateau, Sci. in Chin., Ser. D, 1997, 40: 337.
15. Ding, Z. L., Sun, J. M., Yang, S. L. et al., Preliminary magnetostratigraphy of a thick eolian red clay-loess sequence at Lingtai, the Chinese Loess Plateau, Geophys. Res. Lett., 1998, 25: 1225.
16. Guo, Z. T., Peng, S. Z., Hao, Q. Z. et al., The Relation between the development of arid NW China and ice cover in the North Pole and the uplift of the Tibetan Plateau in Late Tertiary, Quat. Sci. Res. (in Chinese), 1999, 6: 556.
17. An, Z. S., Kutzbach, J. E., Prell, W. L. et al., Evolution of Asian monsoon and phased uplift of the Himalaya-Tibetan plateau since late Miocene times, Nature, 2001, 411: 62.
18. Fang, X. M., Lü, L. Q., Yang, S. L. et al., Loess in Kunlun Mountain and its implications on desert development and Tibetan Plateau uplift in West China, Sci. in Chin., Ser. D, 2002, 45: 289.
19. Pan, B. T., Wu, G. J., Wang, Y. X. et al., Age and genesis of the Shagou River terrace in eastern Qilian Mountains, Chin. Sci. Bull., 2001, 46 (6): 509.
20. Zhang, J. B., Deng, Z. F., Outline of Xinjiang Precipitation (in Chinese). Beijing: Meteor. Press, 1987.
21. Obuluchv, B. A., Loess on the northwest Junggar Basin, Geol. Trans. (in Chinese), 1956(8): 8.
22. Liu, T. S. et al., Loess Deposition in China (in Chinese), Beijing: Sci. Press, 1965.
23. Zhang, H. Y., Wang, H. Z., The loess stratigraphy on the north slope of Tian Shan and the paleoclimate, Arid Region-Xinjiang Quaternary Research Collection (in Chinese), Urumqi: Xinjiang People's Press, 1985, 95—106.
24. Xinjiang Comprehensive Exploration Team of CAS, Xinjiang Quaternary Geology and Environment (in Chinese), Beijing: Science Press, 1995, 11—17, 56—67.
25. Champion, D. E., Lanphere, M. A., Evidence for a new geomagnetic reversal from lava flows in Idaho: discussion of short polarity reversals in the Brunhes and late Matuyama polarity chrons, J. Geophy. Res., 1988, 93: 11667.
26. Zhu, R. X., Kazansky, A., Matasova, G. et al., The loess magnetism of loess deposition in south Siberia, Chin. Sci. Bull. (in Chinese), 2000, 45 (11), 1200.
27. Li, J. J., Evolution of the Environment in northwest China since late Pleistocene, Quat. Sci. Rev. (in Chinese), 1990(3): 197.
28. Fang, X. M, Li, J. J., Van der Voo, R., Paleomagnetic/rockagnetic and grain size evidence for intensified Asian atmospheric circulation since 800 kyrs, Earth Planet Sci. Lett., 1999, 165: 129.

(Received April 16, 2002)